RSC Advances

PAPER

View Article Online
View Journal | View Issue

Cite this: *RSC Adv.*, 2023, **13**, 22358

Tuning the conductance of carbon rings with impurities and electric fields

Carlos Rojas, *[a] A. León,[b] M. Pacheco, [a] Leonor Chico [c] and P. A. Orellana [a]

Received 17th May 2023
Accepted 5th July 2023

DOI: 10.1039/d3ra03297c

rsc.li/rsc-advances

We explore two mechanisms to tune the electronic conductance of carbon atom rings, namely, substitutional impurities and in-plane external electric fields. First-principles calculations and a tight-binding approach are used to model the systems. Two bond configurations are studied, cumulenic and polyynic, which can be relevant depending on the number of carbon atoms in the ring. We find that both impurity substitution and electric field mechanisms allow for modifying the electronic spectrum and transport characteristics. Interestingly, cumulenic and polyynic carbon rings present a different response to these perturbations, which can also be a way to elucidate the bond nature of these structures.

1 Introduction

Single molecules are increasingly considered a potential building block in electronic devices, which holds great promise in miniaturization.[1] Some successes have already been reported along this line, including molecules exhibiting significant on-off current ratios and large negative differential resistance in two-terminal transport, carbon nanotube bridges, and molecular rectifiers.[2] Such setups can eventually be modeled by decomposing the system into coupled molecular subunits that collectively give rise to conducting quantum resonances and antiresonances. The properties of these features determine the transport properties of the system.

By choosing organic molecules, this decomposition can extend device density beyond the limits of conventional small-scale silicon integrated circuits. In this context, carbon-based molecular junctions serve to study a wide variety of charge transport mechanisms since taking advantage of covalent C–C bonds avoids problems such as electromigration while presenting high-temperature stability.[3] Ring-shaped carbon allotropes called cyclo[n]carbons (C_n) present this type of stable configuration of cumulenic, consecutive double bonds.[4,5] In addition, there is a theoretical consensus that a polyynic configuration with alternating single and triple bonds could also represent the lowest energy geometry of these structures for $n = 18$.[6–10] However, this configuration might be different for other numbers of carbon atoms.[11] Due to their high reactivity, cyclo[n]carbons are mostly observed in the gas phase. However, the C_{18} molecule with a polyynic structure[12] was recently synthesized on a surface and characterized with scanning probe microscopies, helping to clarify the controversy about the bond configuration of cyclo[n]carbons. Such breakthrough has also opened the possibility of studying cyclocarbons as possible building blocks in molecular junctions to create small-scale electronic devices. In fact, O-shaped structures as quantum rings have been assembled on semiconductor surfaces.[13] If coherence of the wavefunction is maintained in these structures, quantum transport phenomena as for example persistent currents[14,15] and the Aharonov–Bohm effect[16–18] can be observed in the nanoscale.[19]

Controlling the dimensions, shape, and size of these systems is fundamental and of great technological importance because these parameters are strongly linked to their physical and chemical properties. Moreover, by intentionally doping the material we can modify its electronic, magnetic, and optical properties. It can also be a tool to tailor these devices based on carbon nanostructures.[20] In this spirit, due to the scale of these structures, their manipulation by external means, such as electromagnetic fields, is key for nanotechnological applications. But, at the same time, they can also modify their properties.

A starting point to study this type of system is to connect a conventional conductor to a molecule or some molecular component to study their electron transport properties, as carried out in ref. 11. In this article, we study the electronic transport properties of a carbon atom ring coupled to a quantum wire and two electron reservoirs, considering the two possible bond configurations of cyclo[n]carbons. A thorough study of the ground state configuration, as performed in ref. 21 for isolated rings, is not pursued here. Rather, we focus on the differences produced by weak external perturbations such as adatoms in the ring and electric fields considering both bond configurations, cumulenic and polyynic. Previous studies of these coupled structures show that a single-electron model can

[a]*Departamento de Física, Universidad Técnica Federico Santa María, Casilla 110 V, Valparaíso, Chile. E-mail: carlos.rojasle@usm.cl*

[b]*Instituto de Ciencias Básicas, Facultad de Ingeniería, Universidad Diego Portales, Avda. Ejército 441, Santiago, Chile*

[c]*GISC, Departamento de Física de Materiales, Facultad de Ciencias Físicas, Universidad Complutense de Madrid, 28040 Madrid, Spain*

explain several interesting transport properties, such as the appearance of antiresonances in the conduction spectrum.[11,22–24] In addition, such simplification allows for obtaining analytical expressions for several relevant physical quantities, providing a better insight on the origin of the changes induced by the perturbations.

We focus on conductance changes due to an impurity in the ring and an external electric field, taking as a starting point the pristine conductor-lead structure. We show that the conductance presents an oscillating behavior with resonances and antiresonances with extra peaks due to the influence of these external agents, revealing the energy spectrum of the system. We employ a tight-binding (TB) model to derive our main results, along with first-principles calculations within the density functional theory (DFT) approximation to verify the validity of the single-electron model.

This article is organized as follows: In Sec. 2, we describe the system under consideration and the models used to calculate electronic and transport properties. The discussion of these quantities and comparisons with first-principles calculations are carried out in Sec. 3. Our results and conclusions are summarized in Sec. 4.

2 Geometry and models

The system is schematically depicted in Fig. 1. The central region consists of a ring of M atomic sites and a homogeneous wire of N atomic sites, representing an arrangement of carbon atoms. The ring is attached to a site j in the wire. This central region is connected to two metallic leads modeled as two reservoirs of free states, and an external electric field is applied perpendicular to the wire within the plane of the molecule. A small electric field perpendicular to the plane of the structure would produce a rigid shift of the electronic spectrum, so we focus on a nontrivial configuration that modifies the energy levels of the system and its conductance.

The Hamiltonian of the system within the tight-binding approximation is

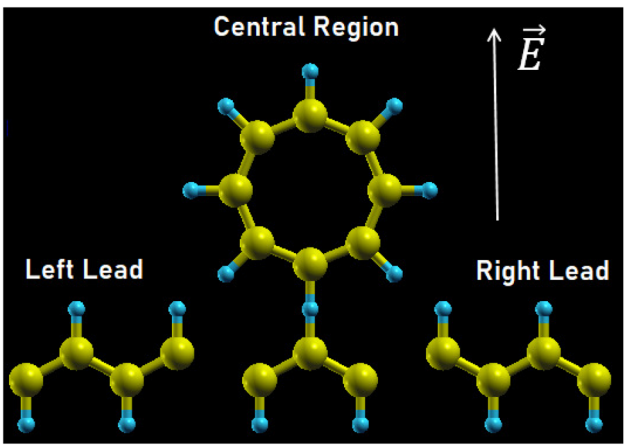

Fig. 1 Schematic representation of the system, where $N = 3$ and $M = 8$.

$$H = H_{\mathrm{w}} + H_{\mathrm{r}} + H_{\mathrm{wr}} + H_{\mathrm{LR}} \tag{1}$$

where H_{w} is the Hamiltonian for the wire,

$$H_{\mathrm{w}} = \sum_{i=1}^{N} \varepsilon_i c_i^{\dagger} c_i - t \sum_{i=1}^{N-1} \left(c_{i+1}^{\dagger} c_i + c_i^{\dagger} c_{i+1} \right). \tag{2}$$

As usual, $c_i^{\dagger}$ (c_i) is the electron creation (annihilation) operator of an electron at site i with energy ε_i. Customarily, we set ε_i equal to zero in one-orbital TB calculations; however, in order to compare TB to DFT approaches, we use this magnitude as a free parameter to fit the results obtained with both methods. In addition, TB results are given as a function of the hopping parameter t, setting its value to 3 eV for comparison to DFT.

The Hamiltonian for the isolated ring H_{r} reads

$$H_{\mathrm{r}} = \sum_{r=1}^{M} (\varepsilon_{r0} + eER\cos(\phi_r)) d_r^{\dagger} d_r - \sum_{r=1}^{M-1} v_r \left(d_{r+1}^{\dagger} d_r + \mathrm{h.c.} \right) \tag{3}$$

where $v_r = v_1, v_2$ if r is odd or even respectively. Here $d_r^{\dagger}$ (d_r) is the electron creation (annihilation) operator of an electron, and $v_{1,2}$ are the hopping terms between the atoms in the ring; ε_{r0} is the contribution to the onsite energy of an atom in the ring without electric field; this energy value is also set to zero for all our calculations except for $\varepsilon_{10} = s$ which represents the onsite energy of the impurity at site $r = 1$. Besides, ε_{r0} was also used as a free parameter to adjust the tight-binding results to DFT calculations. The term next to ε_{r0} is the contribution to the onsite energy due to an in-plane electric field of magnitude E, where R is the magnitude of the position vector for each site in the ring with its origin at the center of the ring and ϕ is the angle between this vector and the external electric field $\vec{E}$. The cumulenic geometry of the ring is modeled by setting $v_1 = v_2$, whereas for the polyynic configuration v_1 and v_2 have different values. The term in the Hamiltonian that describes the coupling between the wire and the ring is

$$H_{\mathrm{wr}} = -V(c_j^{\dagger} d_1 + d_1^{\dagger} c_j), \tag{4}$$

where V is the coupling parameter between site j in the wire and site 1 of the ring. Finally, the coupling to the leads is given by the term

$$H_{\mathrm{LR}} = -\sum_{k_{\mathrm{L}}} V_{k_{\mathrm{L}}}^{\mathrm{L}} \left(f_{k_{\mathrm{L}}}^{\dagger} c_1 + c_1^{\dagger} f_{k_{\mathrm{L}}} \right) \tag{5}$$

$$-\sum_{k_{\mathrm{R}}} V_{k_{\mathrm{R}}}^{\mathrm{R}} \left(f_{k_{\mathrm{R}}}^{\dagger} c_N + c_N^{\dagger} f_{k_{\mathrm{R}}} \right), \tag{6}$$

where $f_{k_q}^{\dagger}$ (f_{k_q}) represents the creation (annihilation) operator of an electron in the continuum with wavevector k_{q}; the couplings between leads and system are given by the parameters $V_{k_{\mathrm{q}}}^{\mathrm{q}}$ with $\mathrm{q} = \mathrm{L}, \mathrm{R}$.

We study the electronic transport properties in the framework of the Landauer approximation, where the two-terminal conductance G at zero temperature is proportional to the total transmission at the Fermi energy E_{F},

$$G = \frac{2e^2}{h} T(E_{\mathrm{F}}). \tag{7}$$

The total transmission is obtained from the Green's functions of each isolated system *via* the Fisher–Lee relation, as detailed in ref. 11.

Lastly, the density of states (DOS) of the ring is also calculated to grasp a better understanding of the transport properties of the system, which is formulated in terms of Green's functions.

$$\rho = -\frac{1}{\pi}\mathrm{Im}\left[\sum_{m=1}^{M}\tilde{G}_{mm}\right] \quad (8)$$

First-principles calculations were also performed using DFT theory employing the GGA-PBE functional as well as transport calculations as implemented in OpenMX.[25,26] We consider this approach to describe correctly the transport properties of our system; indeed, when considering the electron density gradient it takes into account in a precise way the effects of the non-local electron density of the system, which is very important when studying the formation of orbitals in the presence of π bonds. In fact, a previous study shows that this functional has excellent results when describing the transport properties of other carbon-based structures such as carbon nanoribbons, provided that they are not charged, as in this work.[27] Notwithstanding, in order to find the ground state properties of the isolated rings, more sophisticated approaches have been recently used,[21] studying in detail the relative energy between the cumulenic and polyynic forms of C_{4k+2} with k = 4–7 rings found with different calculations methods. We choose not to delve in the precise determination of the stability issues of our more complex leads-ring structure, and focus instead on the differences that both configurations may show in the conductance properties. We have used pseudoatomic orbitals (PAOs) as basis functions to extend the Kohn–Sham wavefunction of a particle. The Kohn–Sham equation is solved in order to obtain the electron density using the fictitious charge density formalism. The minimum energy configuration is found taking energy reorganization into account, by including structural relaxation and polarization effects in the calculation. We have treated the core Coulomb potential with the scheme of pseudopotentials proposed by Morrison, Bylander, and Kleinman.[28] The cutoff energy in all our calculations is 150 Ry with a convergence criterion of 10^{-8} hartree. Furthermore, in all calculations of electrical transport, the method of non-equilibrium Green's function (NEGF) was used.[26]

3 Results and discussion

First of all, for simplicity, we have limited the number of atoms in the chain that connects the ring to the leads, setting $N = 3$. More sites in the chain generate a conduction spectrum with a greater number of resonances, as indicated in,[11] which could hinder the analysis of the effects caused by the ring.

Once we obtain the Green's functions, we calculate the conductance as a function of the energy levels of the wire and the carbon ring. Our previous work[11] showed that the conductance presents an oscillating pattern of resonances and antiresonances; their positions correspond precisely to the energy spectrum of the wire and ring, respectively. Therefore, we can focus on smaller systems (both, coupling chain and carbon ring) in order to study the modifications produced by the external perturbations. We consider different ring sizes, ranging from $M = 4$ to $M = 16$. As commented above, larger rings introduce more features in the spectrum, but the conclusions regarding its origin and modification by external agents remain the same. Likewise, the connection of the ring on the wire has been set to $j = 2$, being a symmetrical point between the contacts. We have verified that in pristine rings changes in the position of the contact merely produce a shift in the energy of the conductance features, leaving our conclusions regarding the transport properties unaltered.

3.1 Impurity effects: cumulenic geometry

The cumulenic structure is modeled by setting all the hopping parameters of the ring equal to t; the impurity is treated as an atom with different onsite energy at an arbitrary position in the ring. We choose a small parameter with respect to the pristine system so perturbation theory is valid. Such weak modification may be due to an adatom on top of the carbon atom of the ring. We have verified that the results do not depend on the particular position of the impurity in the ring. We focus on the study of even rings since C_n molecules with $n = 4k + 2$ (k integer) are predicted to have higher stability.[29–31]

Fig. 2(a) presents the results for the conductance of the system connected to the central atom of the conducting wire for different number atomic sites of the ring M. The system exhibits a series of resonances and antiresonances. The antiresonances that appear at the Fermi level for rings with size $M = 4m$ (with m integer) are related to the spectra of the carbon rings.[11] Furthermore, a resonant peak appears at the Fermi level for $M = 4m$ and additional peaks at some energies where the conductance without the impurity is zero. To analyze the conductance, the energy spectra of the rings derived from the tight-binding model are presented in Fig. 2(b).

The main effect of the impurity is that it breaks the degeneracy of the ring states, justifying the appearance of new resonant peaks in the conductance not only at the Fermi level but at other energies for which degeneracies exist. For instance, there is only one extra peak at the Fermi energy for the ring with $M = 4$, whereas for $M = 8$ there are extra peaks near $\varepsilon = -1.5t$ and $\varepsilon = 1.5t$. Obviously, the larger the ring, the more extra peaks may appear, as can be seen in Fig. 2(a).

Fig. 3(a) displays the conductance zoomed near the Fermi energy for the rings with $M = 4$, 8, 12 and 16 sites with a small impurity. We can see that there are two antiresonances, one exactly at zero and another one shifted to positive energies an amount that depends on the size of the ring M. The pristine ring had two degenerate states at the Fermi level, *i.e.*, at zero energy; the introduction of the impurity breaks this degeneracy. These two states result in two antiresonances in the conductance spectrum at their exact energies. We can predict the energy difference between these two states *via* degenerate perturbation

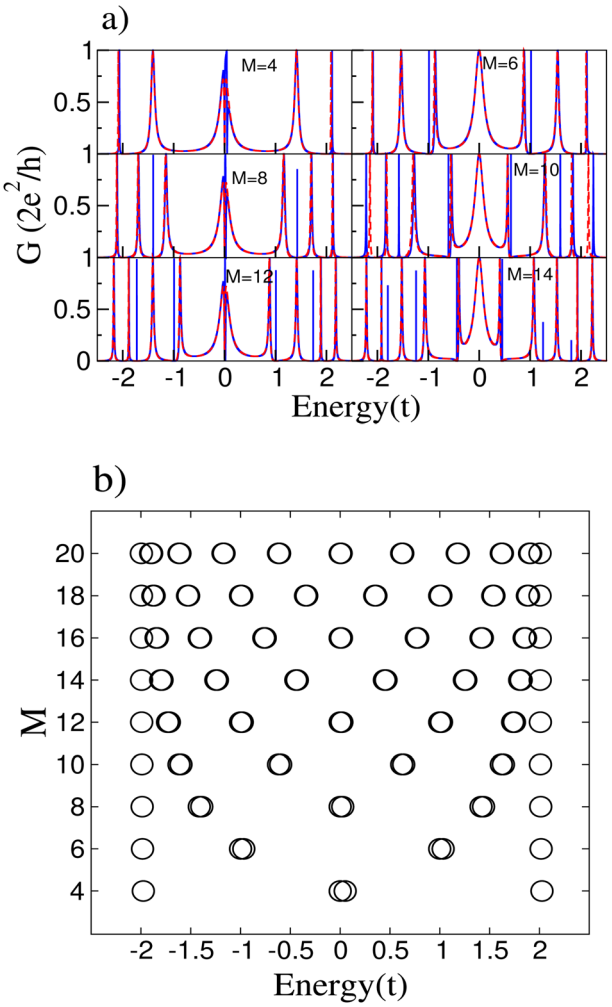

Fig. 2 (a) Conductance *vs.* energy for several rings in the cumulenic configuration with an impurity of onsite energy $s = 0.1t$ (blue) and without impurity (red). (b) Energy spectra of the isolated rings from $M = 4$ to $M = 20$ with an impurity of onsite energy $s = 0.1t$ for the cumulenic configuration in the tight-binding model.

theory. The diagonalization of the perturbation matrix related to the perturbative Hamiltonian $\hat{H}_{\mathrm{p}} = s|1\rangle\langle 1|$ is given by

$$\begin{vmatrix} \hat{H}_{\mathrm{p}_{m,m}} - \varepsilon_n^{(1)} & \hat{H}_{\mathrm{p}_{m,3m}} \\ \hat{H}_{\mathrm{p}_{3m,m}} & \hat{H}_{\mathrm{p}_{3m,3m}} - \varepsilon_n^{(1)} \end{vmatrix} = 0,$$

where the matrix elements $\hat{H}_{\mathrm{p}\alpha,\beta} = \langle\phi_{n_\alpha}|\hat{H}_{\mathrm{p}}|\phi_{n_\beta}\rangle$ being $|\phi_{n_\alpha}\rangle = M^{-1/2}\exp(i2\pi n/M)$ the different eigenstates that correspond to the same energy ε_n with $\alpha, \beta = m, 3m$. The energy corrections for the eigenstates near the Fermi level are $\varepsilon_n^{(1)} = 0$ and $\varepsilon_n^{(1)} = s/2m$. Notice that these energy corrections not only depend on the number of atomic sites but also on the impurity onsite energy s. Obviously, increasing s will also increase the energy splitting of the two states near the Fermi energy, as it is shown in Fig. 3(b). Likewise, weaker impurities produce smaller changes; the differences for couplings smaller than $s = 0.1t$, such as $s = 0.01t$ and $s = 0.001t$, only lie in the fact that the effects are more noticeable for larger values of the site energy s.

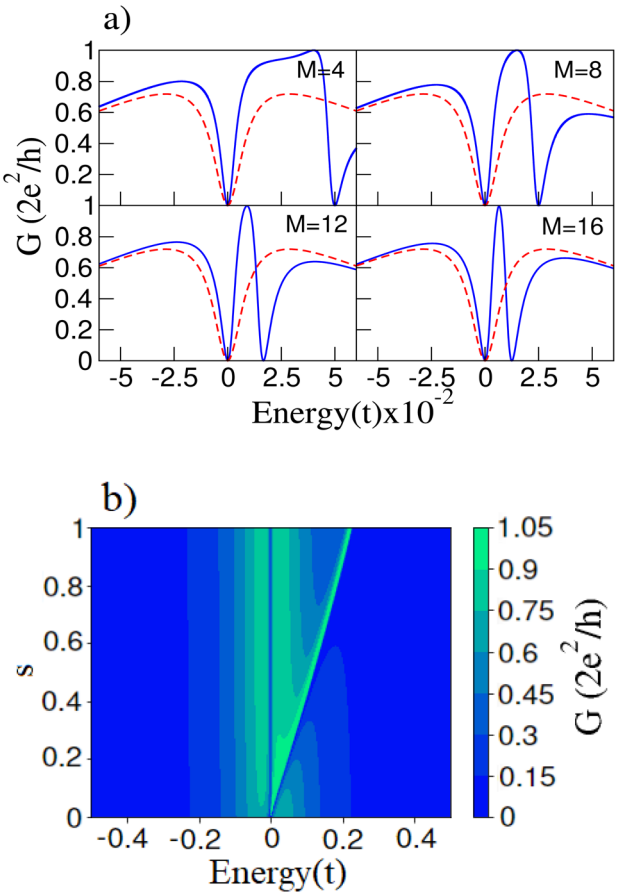

Fig. 3 (a) Conductance *vs.* energy for rings with $M = 4$, $M = 8$, $M = 12$ and $M = 16$ in the cumulenic configuration near the Fermi level with an impurity (blue) of onsite energy $s = 0.1t$ and no impurity (red). (b) Conductance *vs.* energy for different values of the onsite impurity energy s on a ring of $M = 8$ atomic sites.

3.2 Impurity effects: polyynic geometry

The polyynic geometry, with an alternating bond configuration, is modeled by the parameters $v_r = v_1, v_2$, where $v_1 = t$ and $v_2 = 0.75\ t$. Results for the conductance of the system are shown in Fig. 4(a).

In the cumulenic configuration, we observed that the introduction of an impurity removed the degeneracy of the ring states, leading to new resonant peaks in the conductance. We expect the same in the polyynic case, but now the antiresonance at the Fermi level for $M = 4m$ disappears.[11] For this configuration with the impurity, we notice additional resonant peaks in the conductance except for the ring with $M = 4$ sites, which has almost the same spectrum. It can be explained by examining the energy spectra of the isolated rings with the impurity, displayed in 4(b). All the pristine rings have degenerate states, which produce additional conductance resonances if an impurity breaks the degeneracies, except for the $M = 4$ ring. Its energy spectrum does not present degenerate states, leaving its conductance without additional peaks. Closely inspecting the pristine and impurity $M = 4$ ring conductances shows slight differences. Most importantly, it can be noticed a slight

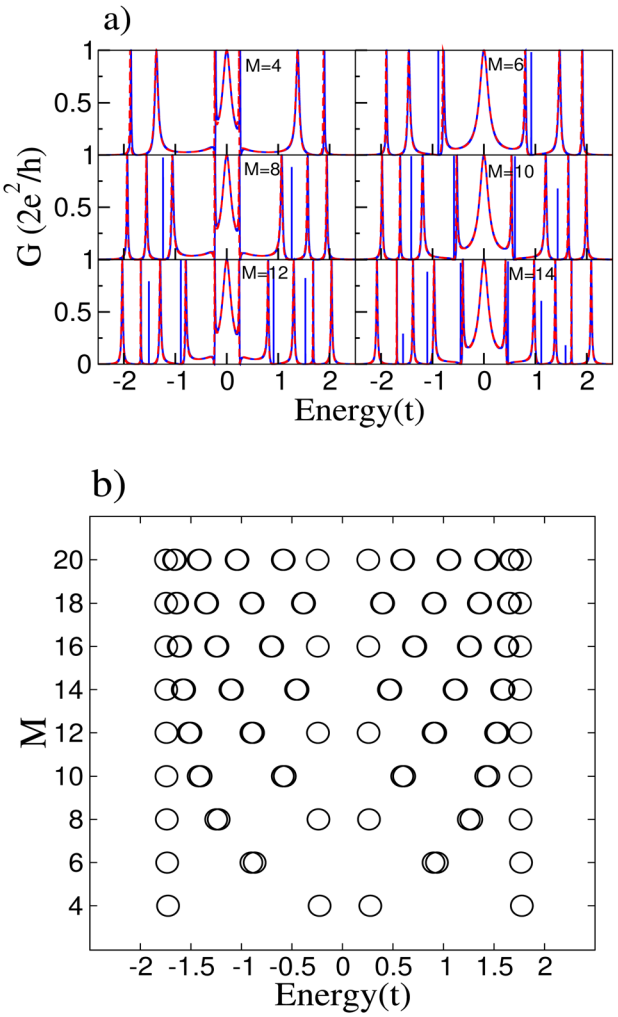

Fig. 4 (a) Conductance *vs.* energy for several rings in the polyynic configuration with an impurity of energy $s = 0.1t$ (blue) and no impurity (red). (b) Energy spectra of the isolated rings from $M = 4$ to $M = 20$ with an impurity of energy $s = 0.1t$ for the polyynic configuration in the tight-binding model.

asymmetry in the conductance near the Fermi energy for the system with the impurity, related to the small changes in the energy spectrum.

3.3 Electric field effects: cumulenic geometry

It is straightforward to show that for the cumulenic configuration, the onsite energy dependence on the electric field E can be expressed as

$$\varepsilon_r = \frac{vE^*M}{2\pi}\cos\left(\frac{2\pi}{M}(r-1)\right), \quad (9)$$

where $r = 1, \ldots, M$ and $E^* = eEa/v$ is the dimensionless electric field strength, as shown previously for a quantum ring.[32] Fig. 5(a) compares the conductance for the system in this configuration for several rings with and without the external electric field. The main effect of the electric field is the appearance of new peaks due to the splitting of the energy levels

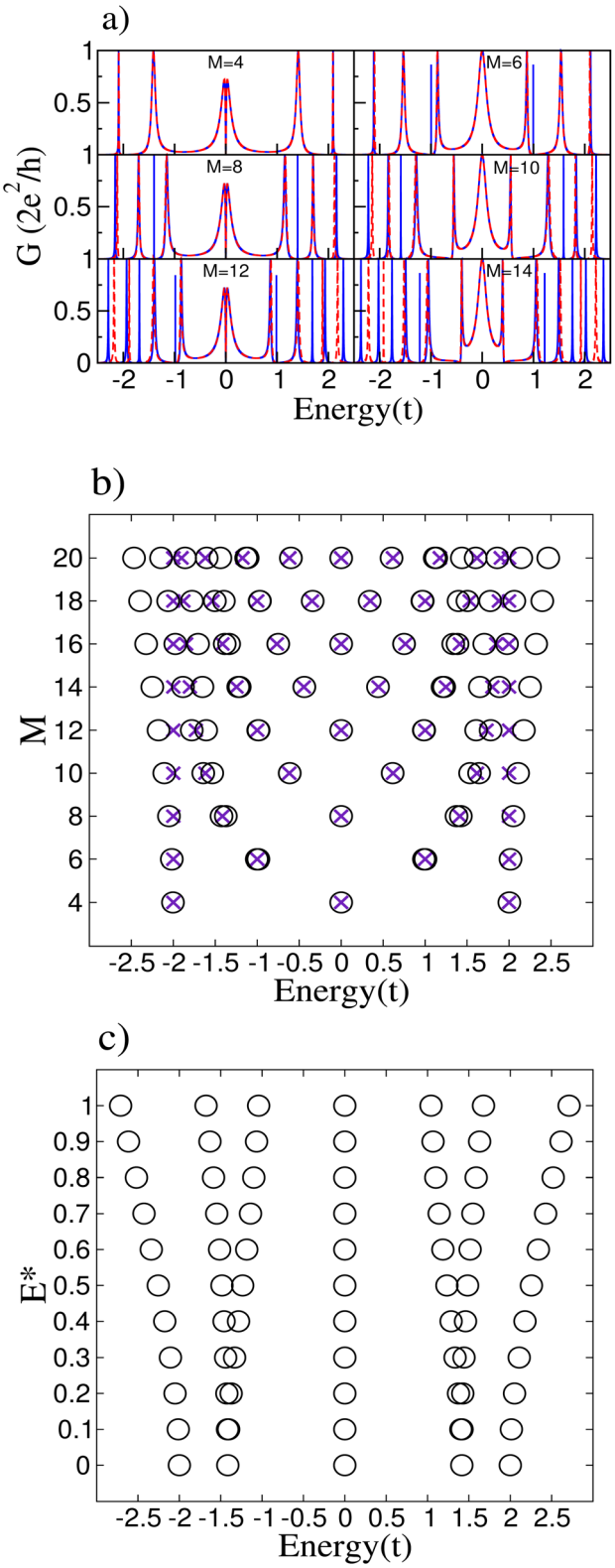

Fig. 5 (a) Conductance *vs.* energy for several rings in the cumulenic configuration with $E^* = 0.2$ (blue) and no electric field (red). (b) Energy spectra of the isolated rings from $M = 4$ to $M = 20$ for the cumulenic configuration in the tight-binding model with $E^* = 0.2$ (circle) and no electric field (X). (c) Variation in the energy spectra of the ring with $M = 8$ sites in the cumulenic configuration for several values of E^*.

of the rings. The removal of the degeneracies is related to the symmetry breaking produced by the electric field, similar to what we observed with the impurity introduction. The largest difference to the impurity case described in Section 3.1 is that with the application of an electric field, there is not a resonant peak at the Fermi level for all the $M = 4m$ rings; this renders all the conductances around the Fermi energy similar to that of the $M = 4$ ring.

In order to explain the electric field results, Fig. 5(b) compares the energy spectra of the isolated rings with and without an electric field. It is clear that the states near the Fermi energy remain unchanged while the degeneracy of the states far from zero energy is broken. On the other hand, for rings with $M = 4m$ with m integer, under an external electric field, a perturbative calculation confirms the invariance of the energy levels at the Fermi level. Following the procedure discussed in Subsection 3.1, it can be easily verified that the energy corrections are all equal to zero, taking into account that in this case, the perturbative Hamiltonian is given by $\hat{H}_{\mathrm{p}} = \sum_{r=1}^{M} \frac{2vE^{*}m}{\pi} \cos\left(\frac{\pi}{2m}(r-1)\right)|r\rangle\langle r|$. Another relevant feature of the electric field on the ring is that the absolute value of the energies increases with the number M of atoms in the ring for those states far from the Fermi energy. Besides, the energy difference between the split states also increases with M. These trends, *i.e.*, larger absolute values of the energies and larger splittings for degenerate levels, also hold for stronger electric fields, as shown in Fig. 5(c) for a $M = 8$ ring.

3.4 Electric field effects: polyynic geometry

For this case, the dependence of the site energy on the field goes as follows.

$$\varepsilon_{lA} = \frac{(v+w)E^{*}M}{4\pi}\cos\left(\frac{4\pi}{M}(l-1)\right), \tag{10}$$

$$\varepsilon_{lB} = \frac{(v+w)E^{*}M}{4\pi}\cos\left(\frac{4\pi}{M}\left(\frac{l(v+w)-w}{v+w}\right)\right), \tag{11}$$

Here the index l stands for the unitary cell containing two atoms A and B, v is the inner hopping of each cell, while the hopping between cells is w, and the dimensionless electric field strength is defined by $E^{*} = eE(a + b)/(v + w)$. Fig. 6(a) shows the comparison of the conductance for the system in the polyynic configuration for several rings with and without the external electric field. As in the cumulenic case, a splitting occurs in the degenerate energy levels of the rings. Note that the conductance for the ring with $M = 4$ sites remains the same as in the cumulenic case since this ring has no degenerate states. Fig. 6(b) compares the energy spectra of the isolated polyynic rings with and without an electric field.

The increase in the absolute value of the energies is not so strong as for the cumulenic case, but the splitting in the degenerate states of this configuration is stronger than for the cumulenic case. Additionally, the energy difference between the states closest to the Fermi level for rings with a number of atoms M multiple of 4 diminishes as the size of the ring

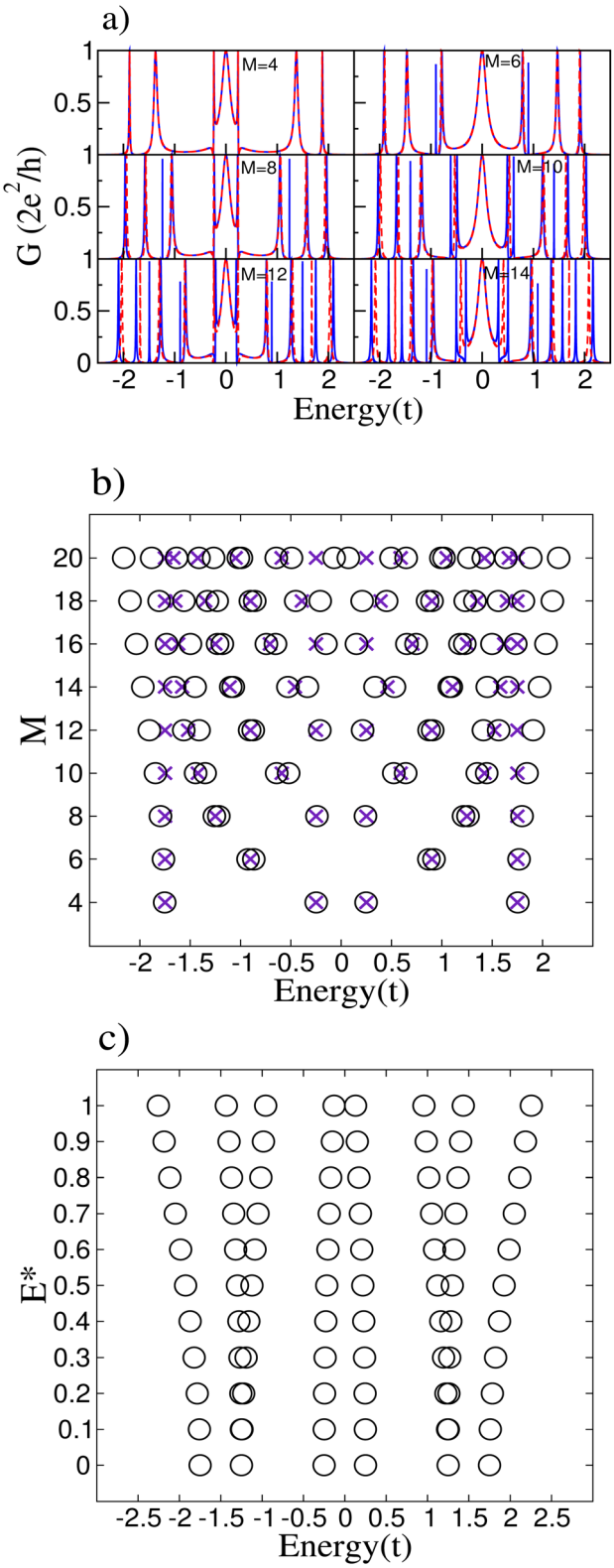

Fig. 6 (a) Conductance *vs.* energy for several rings in the polyynic configuration with $E^{*} = 0.2$ (blue) and no electric field (red). (b) Energy spectra of the isolated rings from $M = 4$ to $M = 20$ for the polyynic configuration in the tight-binding model with $E^{*} = 0.2$ (circle) and no electric field (X). (c) Variation in the energy spectra of the isolated ring with $M = 8$ sites in the polyynic configuration for several values of E^{*}.

increases. The gap also widens when the magnitude of the external electric field increases, as shown in Fig. 6(c).

3.5 Comparison with DFT calculations

DFT calculations were performed to compare with the tight-binding model; we expect the comparison between the two approaches to be valid near the Fermi energy. Fig. 7 shows the conductance for both configurations, cumulenic (a) and polyynic (b), obtained with the two methods. This comparison correctly describes the antiresonance in the Fermi level for cumulenic rings and the new resonant peaks due to the splitting of the degenerate states near 3 eV for the ring with $M = 12$ sites for both ring configurations. The fit is very accurate for positive values of energy.

Fig. 8 compares the energy spectra between TB and DFT for both ring configurations with $M = 8$, all for several values of the electric field strength. Again we find a good agreement near the Fermi energy since there are no changes in the states with zero energy in the cumulenic ring. In addition, notice that the energy difference between the states closest to the Fermi energy decreases as the electric field strength grows stronger for the polyynic configuration in the DFT calculation; both trends are also described correctly within the TB approach.

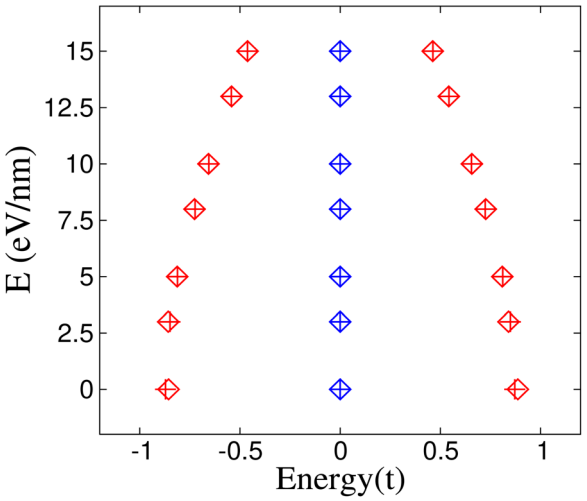

Fig. 8 Comparison of the energy spectra near the Fermi energy for a ring with $M = 12$ sites in both cumulenic (blue) and polyynic (red) configurations obtained with DFT calculations (diamond) and TB model (+).

Lastly, Fig. 9 displays the orbitals for the HOMO and LUMO states for both ring configurations in order to compare with previous work,[11] noting that there is a slight deformation of the orbitals in terms of symmetry when applying the electric field. It is also very remarkable that despite the fact that the energy spectrum of the states with zero energy is not perturbed, there is a change in the wavefunctions, which does reflect the presence of the electric field as an asymmetry in their shape, most clearly seen in Fig. 9(c) and (d). Obviously, one can obtain the

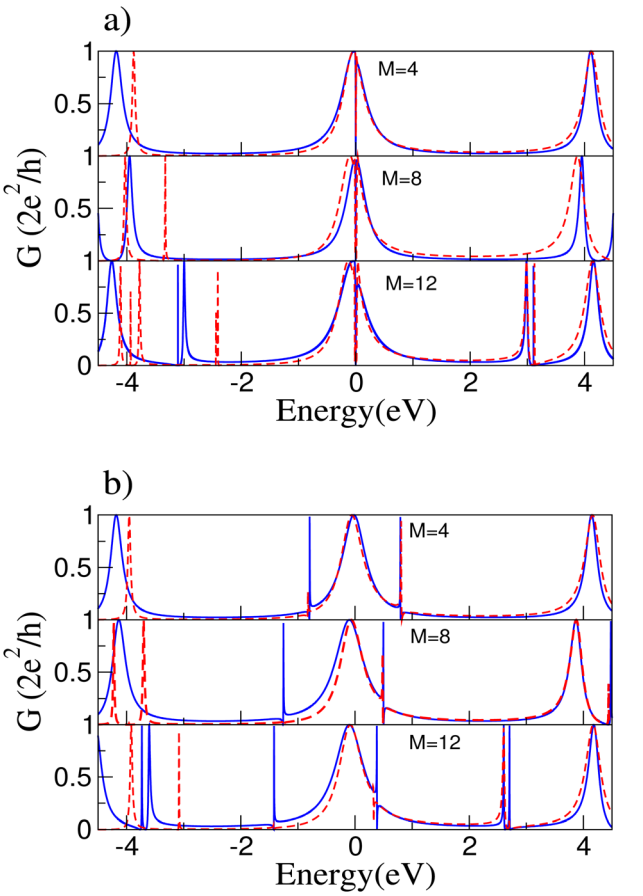

Fig. 7 (a) Comparison of the conductance spectra for rings with $M = 4m$ in the cumulenic configuration between DFT (red) and TB (blue) models. (b) Comparison of the conductance spectra for rings with $M = 4m$ in the polyynic configuration between DFT (red) and TB (blue) models.

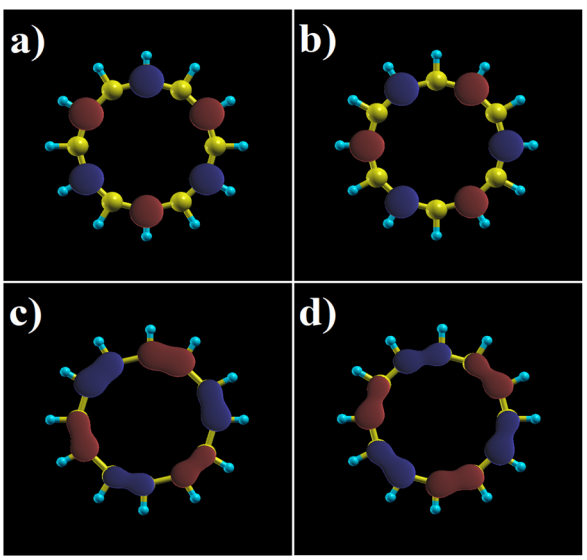

Fig. 9 (a) HOMO and (b) LUMO states for a ring in the cumulenic configuration. (c) HOMO and (d) LUMO states for a ring in the polyynic configuration. Both rings with $M = 12$ atomic sites with an electric field $E = 3$ eV nm^{-1}.

eigenstates that match the shape of the orbitals *via* the diagonalization of the TB Hamiltonian with the presence of the electric field. Also, for weak electric fields, they can be written as a linear combination of the two degenerate states corresponding to the case without an electric field, as it can be graphically inferred by the appearance of the HOMO–LUMO states in Fig. 9.

4 Summary and conclusions

We have explored two ways of tuning the conductance and local density of states of a carbon ring connected to a carbon wire: by introducing an impurity or an external in-plane electric field perpendicular to the wire. We consider two bond configurations, cumulenic and polyynic. We found that the system exhibits an oscillating pattern of resonances and antiresonances related to the discrete spectra of the ring, modified by these external perturbations.

Introducing an impurity atom in the carbon ring breaks the degeneracy of the states, producing new peaks in the conductance spectra for both the cumulenic and polyynic configurations. In the cumulenic case, an additional antiresonance arises near the Fermi energy due to the energy splitting of the degenerate states of the pristine carbon ring. This energy splitting shows a dependence on the onsite energy of the impurity s and the number of atomic sites of the ring M.

Concerning the application of an external electric field, the degeneracy of the states also breaks, although the behavior near the Fermi level remains unaltered in the cumulenic configuration. The energy difference of the states close to the Fermi level in the polyynic configuration decreases as the number of atomic sites in the ring M increases.

The effect is the electric field is more noticeable far from the Fermi energy, especially for larger M.

In summary, we have studied different mechanisms to modify the electronic and transport properties of systems composed of carbon atom rings with different sizes and bond configurations. The difference in their response to external perturbation can be a way to elucidate the nature of the bond in these intriguing systems.

Conflicts of interest

There are no conflicts to declare.

Acknowledgements

This work has been partially supported by Universidad Santa María Grant USM-DGIIP PI-LI 1925 and 1919 and FONDECYT Grants 1201876 and 1211913, Spanish MCIN and AEI, and the European Union under Grant PID2019-106820RB-C21 (MCIN/AEI/FEDER, UE).

Notes and references

1 D. Xiang, X. Wang, C. Jia, T. Lee and X. Guo, Molecular-Scale Electronics: From Concept to Function, *Chem. Rev.*, 2016, **116**, 4318–4440.
2 R. Gupta, J. A. Fereiro, A. Bayat, A. Pritam, M. Zharnikov and P. C. Mondal, Nanoscale molecular rectifiers, *Nat. Rev. Chem.*, 2023, **7**, 106–122.
3 R. L. McCreery, Carbon-Based Molecular Junctions for Practical Molecular Electronics, *Acc. Chem. Res.*, 2022, **55**, 2766–2779.
4 V. Parasuk, J. Almlof and M. W. Feyereisen, *J. Am. Chem. Soc.*, 1991, **113**, 1049–1050.
5 C. Neiss, E. Trushin and A. Görling, The Nature of One-Dimensional Carbon: Polyynic versus Cumulenic, *ChemPhysChem*, 2014, **15**, 2497–2502.
6 T. Torelli and L. Mitas, Electron correlation in C 4 n+ 2 carbon rings: aromatic versus dimerized structures, *Phys. Rev. Lett.*, 2000, **85**, 1702.
7 S. Arulmozhiraja and T. Ohno, CCSD calculations on C 14, C 18, and C 22 carbon clusters, *J. Chem. Phys.*, 2008, **128**, 114301.
8 F. Diederich, Y. Rubin, C. B. Knobler, R. L. Whetten, K. E. Schriver, K. N. Houk and Y. Li, *Science*, 1989, **245**, 1088–1090.
9 G. V. Baryshnikov, R. R. Valiev, A. V. Kuklin, D. Sundholm and H. Ågren, *J. Phys. Chem. Lett.*, 2019, **10**, 6701–6705.
10 A. J. Stasyuk, O. A. Stasyuk, M. Solà and A. A. Voityuk, *Chem. Commun.*, 2020, **56**, 352–355.
11 C. Rojas, A. León, M. Pacheco, L. Chico and P. Orellana, Transport signatures of few-atom carbon rings, *Phys. Chem. Chem. Phys.*, 2022, **24**, 15973–15981.
12 K. Kaiser, L. M. Scriven, F. Schulz, P. Gawel, L. Gross and H. L. Anderson, *Science*, 2019, **365**, 1299–1301.
13 K. Kanisawa, S. Fölsch, *et al.*, Quantum rings engineered by atom manipulation, *Phys. Rev. Lett.*, 2019, **123**, 066801.
14 M. Büttiker, Y. Imry and R. Landauer, Josephson behavior in small normal one-dimensional rings, *Phys. Lett. A*, 1983, **96**, 365–367.
15 D. Mailly, C. Chapelier and A. Benoit, Experimental observation of persistent currents in GaAs-AlGaAs single loop, *Phys. Rev. Lett.*, 1993, **70**, 2020.
16 Y. Aharonov and D. Bohm, Significance of electromagnetic potentials in the quantum theory, *Phys. Rev.*, 1959, **115**, 485.
17 A. Fuhrer, S. Lüscher, T. Ihn, T. Heinzel, K. Ensslin, W. Wegscheider and M. Bichler, Energy spectra of quantum rings, *Nature*, 2001, **413**, 822–825.
18 J. Appenzeller, T. Schäpers, H. Hardtdegen, B. Lengeler and H. Lüth, Aharonov–Bohm effect in quasi-one-dimensional In 0.77 Ga 0.23 As/InP rings, *Phys. Rev. B: Condens. Matter Mater. Phys.*, 1995, **51**, 4336.
19 M. Bayer, M. Korkusinski, P. Hawrylak, T. Gutbrod, M. Michel and A. Forchel, Optical Detection of the Aharonov–Bohm Effect on a Charged Particle in a Nanoscale Quantum Ring, *Phys. Rev. Lett.*, 2003, **90**, 186801.
20 M. Pumera, A. Ambrosi and E. L. K. Chng, Impurities in graphenes and carbon nanotubes and their influence on the redox properties, *Chem. Sci.*, 2012, **3**, 3347–3355.
21 E. Brémond, A. Pérez-Jiménez, C. Adamo and J.-C. Sancho-Garcia, Stability of the polyynic form of C 18, C 22, C 26, and C 30 nanorings: a challenge tackled by range-

separated double-hybrid density functionals, *Phys. Chem. Chem. Phys.*, 2022, **24**, 4515–4525.
22 K. Bao and Y. Zheng, Electronic transport through a quantum-dot ring, *Phys. Rev. B: Condens. Matter Mater. Phys.*, 2006, **73**, 045306.
23 Z. Y. Mijbil, Analytical formula for calculating transmission coefficient of one-dimensional molecules with single impurity, *Solid State Commun.*, 2019, **287**, 13–18.
24 E. Dias and N. Peres, Analytical solution of electronic transport through a benzene molecule using lattice Green's functions, *J. Phys.: Condens. Matter*, 2015, **27**, 145301.
25 J. P. Perdew, K. Burke and M. Ernzerhof, Generalized gradient approximation made simple, *Phys. Rev. Lett.*, 1996, **77**, 3865.
26 T. Ozaki, K. Nishio and H. Kino, Efficient implementation of the nonequilibrium Green function method for electronic transport calculations, *Phys. Rev. B: Condens. Matter Mater. Phys.*, 2010, **81**, 035116.
27 A. León and M. Pacheco, Electronic and dynamics properties of a molecular wire of graphane nanoclusters, *Phys. Lett. A*, 2011, **375**, 4190–4197.
28 I. Morrison, D. Bylander and L. Kleinman, Nonlocal Hermitian norm-conserving Vanderbilt pseudopotential, *Phys. Rev. B: Condens. Matter Mater. Phys.*, 1993, **47**, 6728.
29 G. V. Baryshnikov, R. R. Valiev, R. T. Nasibullin, D. Sundholm, T. Kurten and H. Ågren, *J. Phys. Chem. A*, 2020, **124**, 10849–10855.
30 P. W. Fowler, N. Mizoguchi, D. E. Bean and R. W. Havenith, Double Aromaticity and Ring Currents in All-Carbon Rings, *Chem. - Eur. J.*, 2009, **15**, 6964–6972.
31 K. S. Pitzer and E. Clementi, Large molecules in carbon vapor, *J. Am. Chem. Soc.*, 1959, **81**, 4477–4485.
32 P. Orellana, M. L. de Guevara, M. Pacheco and A. Latge, Conductance and persistent current of a quantum ring coupled to a quantum wire under external fields, *Phys. Rev. B: Condens. Matter Mater. Phys.*, 2003, **68**, 195321.